



HAL
open science

PolSAR Classification based on the SIRV model with a region growing initialization

Pierre Formont, Nicolas Trouvé, Jean-Philippe Ovarlez, Frédéric Pascal,
Gabriel Vasile, Elise Colin-Koeniguer

► **To cite this version:**

Pierre Formont, Nicolas Trouvé, Jean-Philippe Ovarlez, Frédéric Pascal, Gabriel Vasile, et al.. PolSAR Classification based on the SIRV model with a region growing initialization. POLinSAR 2011 - 5th International Workshop on Science and Applications of SAR Polarimetry and Polarimetric Interferometry, Mar 2011, Frascati, Italy. 7 p. hal-00640862

HAL Id: hal-00640862

<https://hal.science/hal-00640862>

Submitted on 14 Nov 2011

HAL is a multi-disciplinary open access archive for the deposit and dissemination of scientific research documents, whether they are published or not. The documents may come from teaching and research institutions in France or abroad, or from public or private research centers.

L'archive ouverte pluridisciplinaire **HAL**, est destinée au dépôt et à la diffusion de documents scientifiques de niveau recherche, publiés ou non, émanant des établissements d'enseignement et de recherche français ou étrangers, des laboratoires publics ou privés.

POLSAR CLASSIFICATION BASED ON THE SIRV MODEL WITH A REGION GROWING INITIALIZATION

Pierre Formont^{*1,2}, Nicolas Trouvé¹, Jean-Philippe Ovarlez^{1,2}, Frédéric Pascal², Gabriel Vasile³, and Elise Colin-Koeniguer¹

¹ONERA DEMR/TSI, Chemin de la Hunière, 91430 Palaiseau Cedex, France, jean-philippe.ovarlez@onera.fr,
nicolas.trouve@onera.fr, elise.koeniguer@onera.fr

²SONDRA, 3 rue Joliot Curie, 91192 Gif-sur-Yvette Cedex, France, pierre.formont@supelec.fr, frederic.pascal@onera.fr

³GIPSA-lab, 961 rue de la Houille Blanche, BP 46, 38402 Grenoble Cedex, France,
gabriel.vasile@gipsa-lab.grenoble-inp.fr

ABSTRACT

Polarimetry has been studied for many years in SAR. Due to the enormous quantity of SAR images acquired by satellites or airborne systems, there is an evident need for efficient automatic analysis tools. Classification algorithms are one of the main applications for PolSAR data. Nowadays, fully polarimetric high resolution sensors can commonly reach up to decimeter resolutions. This yields a higher heterogeneity in the clutter, especially in urban areas, where the clutter can no longer be modeled as a Gaussian process. Recent advances in the field of SIRV (Spherically Invariant Random Vectors) allow the modeling of non-Gaussian clutter as a compound Gaussian process. In this paper, we propose to apply a region growing process as an initialization to a SIRV based classification technique. As the region growing process is shape constrained, spatial features are better delineated and the samples used for the estimation of the coherency matrices are more adapted. Then a statistical clustering technique adapted to the SIRV model is applied to retrieve similarities between regions in the whole image.

Key words: SAR, polarimetry, non-Gaussian, classification, segmentation.

1. INTRODUCTION

Polarimetric unsupervised classification technics have been a topic of interest for the past decade. Most of the classification algorithms involve classical polarimetric decomposition [1] [2] as an initial image classification and then apply an iterative and self converging statistical classification (K-mean Wishart). Among them the most commonly used is known as H-Alpha Wishart classification. It was shown in [3] that the H-Alpha initialisation is not meaningful as the criterion used to describe the data

in the H-Alpha space is drastically different from the ones used afterwards in the Wishart clustering process. In the present paper we propose instead to apply a spatial image partition, results of a region growing process, to initialize the classification algorithm. The principle of the hierarchical region growing method is explained by the flowchart in Fig. 1. It is a recursive algorithm that involves iterative region merging based on statistical considerations and, in our case, shape control. The initial partition is usually a thin grid partition of the studied image; each region seeds the region growth and, at every step, the two regions with the closest statistical and shape criteria are merged. Defining an appropriate stop criterion is difficult when region growing is applied to segmentation/classification. Here, as the goal is to provide a good estimation of the PolSAR parameters for each region, we end the iterative process when an average region size has been reached.

The proposed classification algorithm involves the same statistical model as in [3], but this time a K-means++ algorithm [4] is adapted to the SIRV distribution model and applied after the initial image partition.

This paper is organized as follows: in the first part the region growing algorithm is briefly described and results on a PolSAR image from Toulouse are presented. Then the statistical framework and the classification algorithm are described and tested on an image sample. Finally, results on a large image acquired by the ONERA RAMSES system at X band are presented.

2. STATISTICAL DISTANCES FOR REGION GROWING

In order to implement our region growing process, we must define a statistical criteria and shape constraints. A statistical criterion requires the definition of a statistical distance based on a hypothesis test and a distribution model to describe our measurements. Based on theoretical and experimental considerations, the Kullback Leibler

^{*}The author would like to thank the DGA for funding this research.

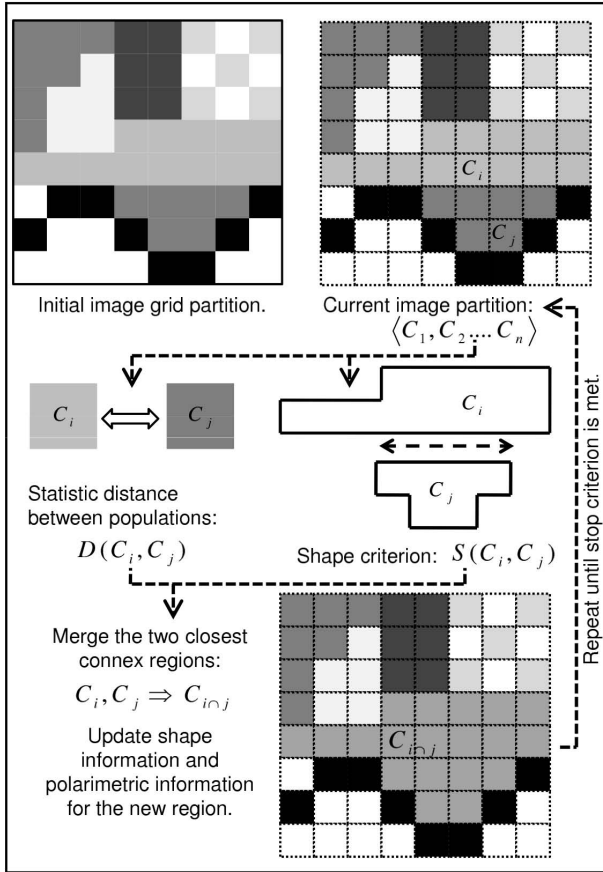


Figure 1. Recursive principle of the hierarchical region growing method.

divergence was chosen for slightly outperforming other classical distances in the given range of sample number and dimension.

The previous hierarchical polarimetric segmentation algorithms used on PolSAR images [5, 6] and presented in the literature mainly focus on the texture information, with ever increasing model precision. However, they remain highly dependent on the a priori texture model. In most cases, as the complexity of the model increases, so does the computing time. Since very high resolution sensors produce very large volumes of data, practical applications must be cautiously set up to prevent unrealistic time costs. Hence the SIRV model, introduced to polarimetry by Vasile and Ovarlez [7], was chosen to handle non gaussian high resolution sensors data while preserving acceptable time efficiency.

3. SHAPE CONSTRAINT

Shape information can play a determinant role in a segmentation process. When studying an image, human operators can make full use of their a priori shape knowledge to identify items of interest. In a SAR image,

even an untrained human eye can easily identify buildings or roads, because of their rectangular shape or linearity. An expert eye could even use its knowledge on backscattering effects such as double bounces and shadows to improve the interpretation of building shapes and sizes. Shape constraint region growing techniques use that prior knowledge on the shape to guide the growth of the region during the segmentation process. Depending on the concerned application, more specific shape rules can be introduced. Beaulieu and Touzi already introduced shape information for PolSAR segmentation [5] where they have shown noticeable improvement over unsupervised techniques.

Handling multiple shape rules can be a difficult task, as increasing the number of rules can often lead to interference and unexpected segmentation behavior. The relative weight between the statistical distance and the shape rule criterion is also a tricky parameter. In this paper we propose to use fuzzy logic and fuzzy inference systems to handle shape rules, their parameters and their relative weights. The main advantage of fuzzy logic is its simplicity, as it permits to translate if-then rules on linguistic variables into fuzzy shape rules and parameters. Computational effort is also very low if the shape parameter estimation remains simple enough. System adjustment by tuning rule weights and settings is also much easier to handle compared to alternatives such as trained networks.

3.1. Shape rules examples

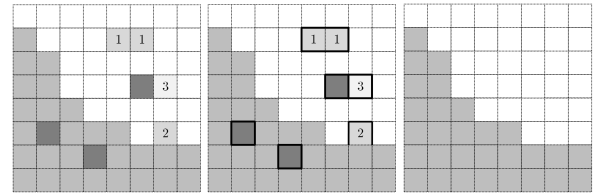


Figure 2. "Small" regions having a "High" Boundary / Perimeter ratio lead to a "Very Low" shape criterion. They are then merged with their surrounding neighbors even if the statistical distance remains too high.

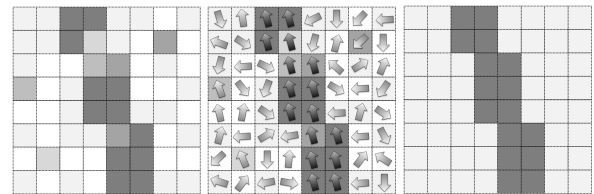


Figure 3. "Small" regions having a "Low" linear angle difference lead to a "Low" shape criterion. They are merged together even if the statistical distance is slightly too high to enhance and preserve linear items.

In this paper, two rule examples are briefly explained on Fig. 2 and Fig. 3. More details regarding the shape rules

design and balance can be found in a more detailed paper [8].

3.2. Results on PolSAR images

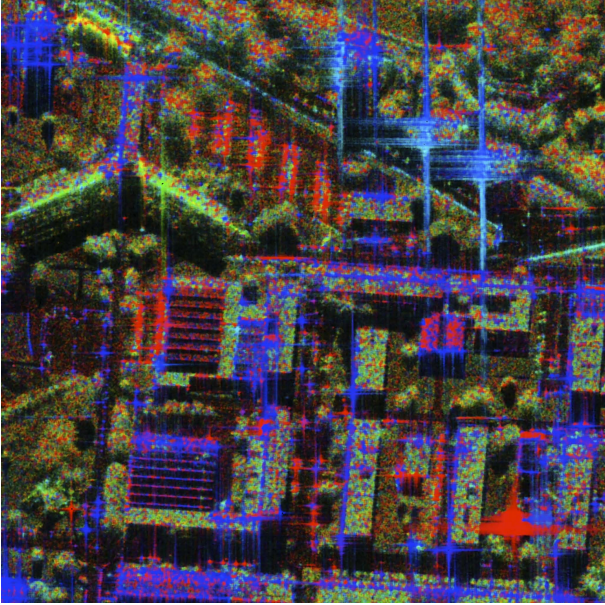


Figure 4. PolSAR X-band image from SETHI over Toulouse. Pauli representation of the coherency matrix estimated on the initial image by a 5×5 averaging box-car).

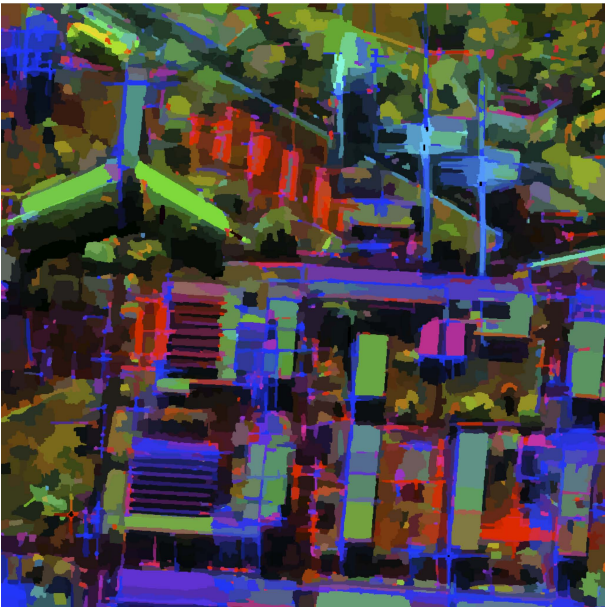


Figure 5. PolSAR X-band image from SETHI over Toulouse. Pauli representation of the coherency matrix estimated on the region growing segmentation results.

4. THE SIRV MODEL

Spherically Invariant Random Vectors (SIRV) were first introduced by Yao [9] for estimation and detection in communication theory. A SIRV is a compound Gaussian vector, defined as the product of a m -dimensional complex circular Gaussian vector \mathbf{x} and the square root of a positive scalar random variable τ . Then the target vector \mathbf{k} can be rewritten as:

$$\mathbf{k} = \sqrt{\tau} \mathbf{x} \quad (1)$$

where $\mathbf{x} \sim \mathcal{N}(\mathbf{0}, \mathbf{M})$.

This models allows to take the heterogeneity of the scene into account thanks to the texture variable τ . Indeed, the texture models the local variations of power from cell to cell, that are the consequences of the heterogeneity.

The speckle variable \mathbf{x} , on the other hand, contains the polarimetric information through the covariance matrix \mathbf{M} that describes it.

The texture Probability Density Function (PDF) is not explicitly specified. This results in a large class of stochastic processes describable by this model, including the Gaussian one. Other classical distributions the SIRV model can describe are the K-distribution for a Gamma distributed texture, Chi, Rayleigh, Weibull or Rician PDFs [10]. This model has furthermore been validated by numerous measurements campaigns [11]. With the SIRV model and a deterministic texture assumption, Gini et al. [12] derived the Maximum Likelihood (ML) estimate of the covariance matrix \mathbf{M} as the solution of the following equation:

$$\widehat{\mathbf{M}}_{FPE} = f(\mathbf{M}) = \frac{m}{N} \sum_{i=1}^N \frac{\mathbf{k}_i \mathbf{k}_i^H}{\mathbf{k}_i^H \widehat{\mathbf{M}}_{FPE}^{-1} \mathbf{k}_i}. \quad (2)$$

Conte et al. proposed in [13] a recursive algorithm to estimate the Fixed Point Estimate (FPE), $\widehat{\mathbf{M}}_{FPE}$, as the fixed point of the function f of Eq. (2). This work was completed in [12] [13] to extend this estimation scheme to the stochastic texture hypothesis. Under this assumption, the FPE is an Approximate ML estimator. Pascal et al. recently established very important properties of the recursive algorithm in [14]. The existence and uniqueness of the solution is proven, as well as the convergence whatever the initialisation. In [15], properties of the FPE are provided: it is unbiased, consistent and asymptotically Wishart-distributed.

When replacing the scattering vectors \mathbf{k}_i in Eq. (2) by their expression of Eq. (1), the FPE becomes:

$$\widehat{\mathbf{M}}_{FPE} = f(\mathbf{M}) = \frac{m}{N} \sum_{i=1}^N \frac{\mathbf{x}_i \mathbf{x}_i^H}{\mathbf{x}_i^H \widehat{\mathbf{M}}_{FPE}^{-1} \mathbf{x}_i}. \quad (3)$$

thus removing the texture information from the expression of $\widehat{\mathbf{M}}_{FPE}$.

5. CLASSIFICATION PROCEDURE

5.1. Statistical Test of Equality of Covariance Matrices

The goal is to decide if the covariance matrices \mathbf{T}_1 and \mathbf{T}_2 from 2 different populations are equal. The resulting binary hypothesis test can be written as:

$$\begin{cases} H_0 : \mathbf{T}_1 = \mathbf{T}_2 \\ H_1 : \mathbf{T}_1 \neq \mathbf{T}_2 \end{cases}$$

The resulting test statistic is given by the following equation:

$$\lambda = \frac{|\widehat{\mathbf{T}}_1|^{\frac{N_1}{2}} |\widehat{\mathbf{T}}_2|^{\frac{N_2}{2}}}{|\widehat{\mathbf{T}}|^{\frac{N}{2}}} \quad (4)$$

where N_i is the size of the population i and $\widehat{\mathbf{T}} = \frac{1}{N}(N_1\widehat{\mathbf{T}}_1 + N_2\widehat{\mathbf{T}}_2)$.

Bartlett proposed in [16] alternative exponents by replacing the samples size by the degree of freedom of the estimators $\widehat{\mathbf{T}}_i$. Eq. (4) then becomes:

$$t = \frac{|\widehat{\mathbf{T}}_1|^{\frac{\nu_1}{2}} |\widehat{\mathbf{T}}_2|^{\frac{\nu_2}{2}}}{|\widehat{\mathbf{T}}|^{\frac{\nu_t}{2}}} \quad (5)$$

where $\nu_i = N_i - 1$ are the degrees of freedom of $\widehat{\mathbf{T}}_i$ and $\nu_t = N - 2$, the degree of freedom of $\widehat{\mathbf{T}}$.

Box proposed in [17] a modification of the test statistic t in:

$$u = -2(1 - c_1) \ln(t) \sim \chi^2\left(\frac{1}{2}(k-1)m(m+1)\right) \quad (6)$$

where $\chi^2(a)$ denotes the χ^2 distribution with a degrees of freedom and

$$c_1 = \left(\sum_{i=1}^k \frac{1}{\nu_i} - \frac{1}{\sum_{i=1}^k \nu_i} \right) \left(\frac{2m^2 + 3m - 1}{6(k-1)(m+1)} \right)$$

5.2. Algorithm

A k-means++ algorithm[4] is employed for the classification procedure. It is a slight modification of the k-means algorithm in its initialization process. Instead of choosing the initial class centers at random among the data points, the idea is to spread them as far away as possible from one another. The initialization procedure is as follows:

1. The first center is chosen at random among the data points.
2. For each data point, compute the distance between itself and its closest class center.
3. Choose a new class center with a probability weighted by the square of the distance computed in step 2. This way, data points farther away have a higher chance to be selected as class centers.
4. Repeat steps 2 and 3 until the desired number of class has been reached.

In our case, the data points are the segments resulting from the region growing procedure of Section II. They are represented by the covariance matrices $\widehat{\mathbf{M}}_{FP}$ estimated using all the scattering vectors belonging to the segment. The distance used in step 2 is the test statistic of Eq. (6).

After the initialization, a standard k-means procedure is applied until convergence, that is when no segment switch classes during an iteration.

The complete classification procedure is described below:

1. Apply the region growing procedure to a PolSAR image.
2. Compute the covariance matrices of each segment using Eq. (2).
3. Initialize the class centers with the above procedure with the desired number of classes.
4. For each segment, compute its distance to each class center using Eq. (6) and take the minimum of those distance.
5. If this minimum is below the threshold given by the χ^2 -approximation, assign the segment to the corresponding class. Else assign the segment to a rejection class.
6. Recompute the class centers as the mean of the covariance matrices of all the segments belonging to the class.
7. Repeat steps 4-6 until convergence.

6. RESULTS ON REAL DATA

We present the results obtained on two data sets, the first one being a subset of the second, larger one. They were acquired in X-band by the ONERA RAMSES system in the region of Brétigny, France. The resolution is approximately 1.3m both in range and azimuth.

6.1. First dataset

The first dataset is a 451x451 pixels image extracted from the larger, second dataset. Fig. 6 provides a representation of this image in the Pauli basis.



Figure 6. Pauli representation of the first dataset.

The region growing procedure results are presented on Fig. 7.

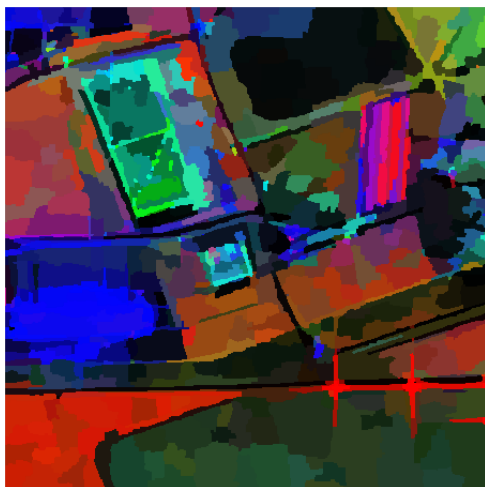


Figure 7. Pauli representation of the region growing results ($HH+VV/HH-VV/HV$).

On Fig. 8 are represented the results of the classification procedure.

Fig. 8 (a) represents the results of the classification procedure using the SCM and Fig. 8 (b) with the FPE. Using the SCM, all the man-made structures of the image (buildings, parking lot on the right) are inside the rejection class. Using the FPE, the rejection class is much smaller and the buildings stand out much better and in

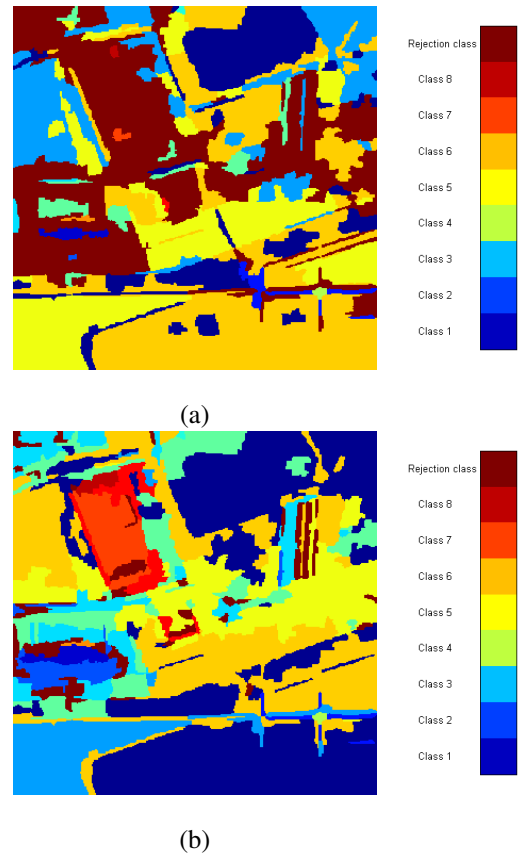


Figure 8. Classification procedure with 8 classes and associated colormaps : (a) with SCM, (b) with FPE

separate classes. The classification in heterogeneous areas is then improved

6.2. Second dataset

The second data set is a much larger image (1500x3400 pixels) of the same area. The segmentation results on this image are represented on Fig. 9.

Fig. 10 shows the result of the classification procedure on this larger dataset using the FPE and 16 classes.

There is a good adequation between the Pauli representation of Fig. 9 and the classification results of Fig. 10. Areas with a dominance of red (surface) are merged in the class appearing in red after classification. Buildings and urban areas are mostly represented by the blue classes. Some segments are classified in blue and purple in the bands at the top and at the bottom of the image. This is due to the fact that there is very little power so the measurements have little meaning. The rest of the image is quite well separated as well. A formal classification accuracy can not be performed because no ground truth is available for this data set.

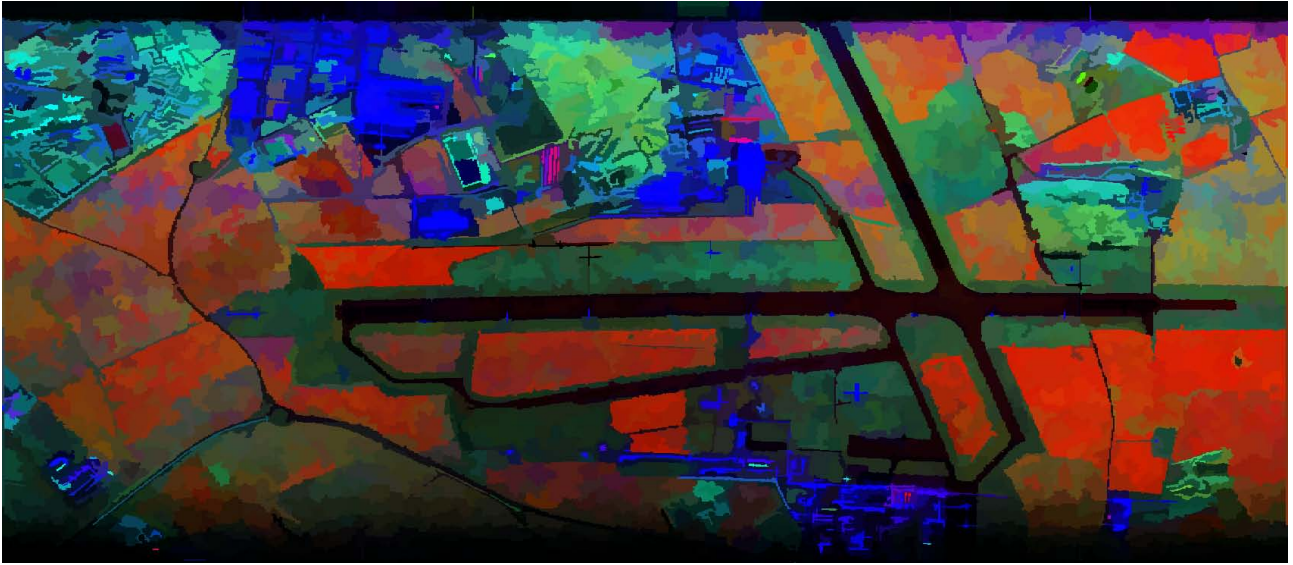


Figure 9. Region growing results in the Pauli basis ($HH+VV$ / $HH-VV$ / HV).

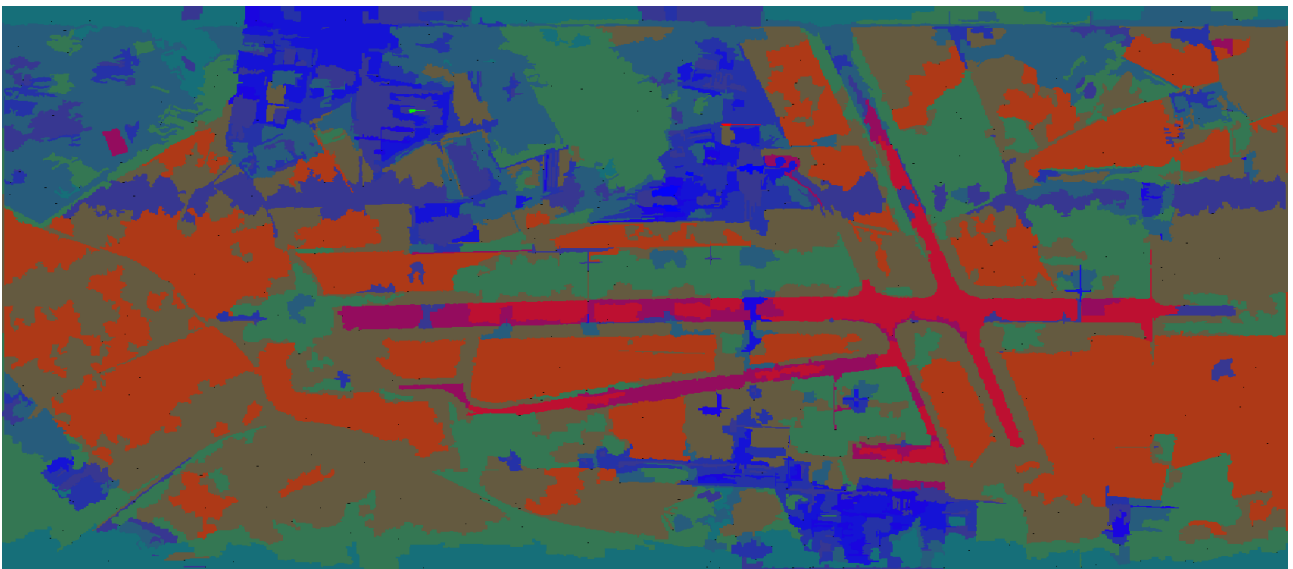


Figure 10. Classification results with 16 classes and the FPE.

7. CONCLUSION

This paper presented a classification procedure for high resolution polarimetric SAR images. First, a region-growing method to cluster pixels thanks to their polarimetric properties under shape constraints was described. Then, a statistical model adapted to the heterogeneous nature of high resolution polarimetric SAR images was presented, along with the statistical test used in the classification process. The algorithms have been tested on real data and show the interest of using such a model. The region-growing method allows to reduce drastically both the computation time and the randomness of the subsequent classification algorithm, thus making it much more robust.

REFERENCES

1. S. R. Cloude and E. Pottier, "An Entropy Based Classification Scheme for Land Applications of Polarimetric SAR", *IEEE Trans. on Geoscience and Remote Sensing*, Vol. 35, No. 1, pp.68-78, Jan. 1997.
2. A. Freeman and S. Durden, "A Three-Component Scattering Model for Polarimetric SAR Data", *IEEE Trans.-GRS*, Vol. 36, No. 3, pp. 963-973, May 1998.
3. P. Formont, F. Pascal, G. Vasile, J.-P. Ovarlez and L. Ferro-Famil, "Statistical Classification for Heterogeneous Polarimetric SAR Images", to appear in *Journal of Selected Topics in Signal Processing*, June 2011.
4. D. Arthur and S. Vassilvitskii, "K-Means++: the Advantages of Careful Seeding", *Proceedings of the 18th annual ACM-SIAM symposium on Discrete algorithms*, pp. 1027-1035, 2007.
5. J.M. Beaulieu and R. Touzi, "Segmentation of textured polarimetric SAR scenes by likelihood approximation", *IEEE Trans.-GRS*, Vol. 42, No. 10, 2004.
6. L. Bombrun and J.M. Beaulieu, "Fisher distribution for texture modeling of polarimetric SAR data", *IEEE GRSL*, Vol. 5, No. 3, 2008.
7. G. Vasile, J.-P. Ovarlez, F. Pascal and M. Gay, "Estimation of the normalized coherency matrix through the SIRV model. Application to high resolution POLSAR data", *POLinSAR 2009, European Space Agency, Frascati, Italy*, 2009.
8. N. Trouvé, E. Colin-Koeniguer and H. Cantalloube, "Shape Constraint Region Growing Process and Application to 3D Rendering of High Resolution Urban Images", *POLinSAR 2011, European Space Agency, Frascati, Italy*, 2011.
9. K. Yao, "A representation theorem and its applications to spherically-invariant random processes", *IEEE Transactions on Information Theory*, Vol. 19, No. 5, pp. 600-608, 1973.
10. M. Rangaswamy, D. D. Weiner and A. Ozturk, "Computer generation of correlated non-Gaussian radar clutter", *IEEE Trans.-AES*, Vol. 31, No. 1, pp. 106-166, 1995.
11. J.B. Billingsley, "Ground clutter measurements for surface-sited radar", MIT, Tech. Rep. 780, February 1993
12. F. Gini and M. V. Greco, "Covariance Matrix Estimation for CFAR Detection in Correlated Heavy Tailed Clutter", *Signal Processing*, Vol. 82, No. 12, pp. 1847-1859, 2002.
13. E. Conte, A. DeMaio, and G. Ricci, "Recursive Estimation of the Covariance Matrix of a Compound-Gaussian Process and its Application to Adaptive CFAR Detection", *IEEE Trans. on Image Processing*, Vol. 50, No. 8, pp. 1908-1915, 2002.
14. F. Pascal, Y. Chitour, J.P. Ovarlez, P. Forster and P. Larzabal, "Covariance Structure Maximum Likelihood Estimates in Compound Gaussian Noise: Existence and Algorithm Analysis", *IEEE Trans. on SP*, Vol. 56, No. 1, pp. 34-48, Jan. 2008.
15. F. Pascal, P. Forster, J.P. Ovarlez and P. Larzabal, "Performance Analysis of Covariance Matrix Estimates in an Impulsive Noise", *IEEE Trans. on SP*, Vol. 56, No. 6, pp. 2206-2217, Jun. 2008.
16. M.S. Bartlett, "Properties of Sufficiency and Statistical Tests", *Proc. of the Royal Society of London*, Vol. 160, pp. 268-282, 1937.
17. G.E.P. Box, "A General Distribution Theory for a Class of Likelihood Criteria", *Biometrika*, Vol. 36, 1949.